國立交通大學

電子工程學系電子研究所

碩 士 論 文

仿酢漿草結構為感測振膜之高性能音源定位麥克風的設計與製作

Design and Fabrication of High Performance Sound-Localized Microphone Using Oxalis-like Sensing Diaphragm

研 究 生：景 文 澔

指導教授：鄭 裕 庭　教授

中 華 民 國 九 十 五 年 十 月

仿酢漿草結構為感測振膜之高性能音源定位麥克風的設計與製作

Design and Fabrication of High Performance Sound-Localized Microphone Using Oxalis-like Sensing Diaphragm

研 究 生：景文澔　　Student：Wen-Hao Ching

指導教授：鄭裕庭　　Advisor：Yu-Ting Cheng

國 立 交 通 大 學

電子工程學系電子研究所

碩 士 論 文

A Thesis

Submitted to Department of Electronics Engineering & Institute of Electronics

College of Electrical and Computer Engineering

National Chiao-Tung University

in Partial Fulfillment of the Requirements

for the Degree of Master

in

Electronics Engineering

October 2006

Hsinchu, Taiwan, Republic of China

中華民國九十五年十月

仿酢漿草結構為感測振膜之高性能音源定位麥克風的設計與製作

學生：景文澔　　指導教授：鄭裕庭教授

國立交通大學電子工程學系暨電子研究所碩士班

摘　　要

科學家發現中文學名為奧米亞棕蠅的聽覺器官可經由一種獨特的橋型結構將振膜相互連接來定位出微小的聲音梯度。在此篇論文中，我們利用中央平衡環支撐式圓形結構 [5-8] 並且模仿酢漿草的結構，提出了一個全新發展的微機械仿生物式麥克風。這種仿酢漿草的振膜能夠經由減少感測振膜之間的交互影響來改善其位移量，並且能夠利用中央平衡環結構的最佳化設計來提升音源定位的能力。此外，相較於中央平衡環支撐式圓形振膜的設計，仿酢漿草的設計可提供 3.7 倍大的淨位移量，而且，仿酢漿草的振膜能表現出小於 10 度的空間分辨率。文中所有的設計與模擬是利用有限元素分析法的模擬軟體 ANSYS 來完成的。最後利用標準的 MUMPs (Multi-User MEMS Precesses)製程以及表面微加工技術製作出單一晶片的仿生物式麥克風。

Design and Fabrication of High Performance Sound-Localized Microphone Using Oxalis-like Sensing Diaphragm

Student : Wen-Hao Ching Advisor : Yu-Ting Cheng

Department of Electronics Engineering & Institute of Electronics
National Chiao Tung University

Abstract

Researchers found the Ormia Ochracea's auditory organ can locate a small sound gradient via a unique intertympanal bridge structure. In this thesis, we propose a newly developed micromachined biomimetic microphone by utilizing the central gimbals-support circular structure [5-8], and mimicking the structure of the oxalis. The oxalis-like diaphragm can not only improve the displacement by decoupling the sensing diaphragm but also enhance the capability of sound source localization with the optimum design of the central gimbals structure. Moreover, the net displacement of the diaphragm with the oxalis-like design has 3.7 times larger than that of the diaphragm with the central gimbals-support circular diaphragm design, and the oxalis-like diaphragm performs the spatial resolution with opening angle smaller than 10 degrees. The design and FEM simulation are analyzed by ANSYS simulator. The process of the single-wafer biomimetic microphone is fabricated by the standard Multi-User MEMS Processes (MUMPs) with three poly-silicon layers and two sacrificial layers.

Acknowledgments

First and foremost I would like to thank my advisor, Dr. Yu-Ting Cheng, for the thoughtful guidance, encouragement, and valuable discussion during the course of this study. Also, I would like to thank all my colleagues of our group in the past two years. Moreover, I would like to express my appreciations to the Nano Facility Center of National Chiao-Tung University, Prof. Hsu's group in Department of Mechanical Engineering in National Chiao-Tung University for providing technical supports and measurement facilities.

This work was supported by the NSC 95-2220-E-009-036 project and in part by MediaTek research center and FY95 ITRI/STC/JDRC at National Chiao Tung University.

誌　謝

首先要感謝我的家人，謝謝辛苦賺錢的老爸，「爸，沒有一個員工早上六點就起床上班的，連周未也是如此！！」，謝謝一直伸手要零用錢的老媽，「媽，家裡的東西不要再捨不得丟了，我買新的給妳!！！」還有謝謝一起亂花錢的老哥，「哥，一起努力賺錢吧！！」。謝謝你們從小到大對我的包容與支持。對於一個生長在幸福家庭的小孩，卻不懂得珍惜這一切，但在人生的另一個重要的開始，還是要跟你們說一聲謝謝，沒辦法早點畢業，讓你們擔心了。

另外要感謝我的指導老師鄭裕庭教授，謝謝你在這段期間對我的指導，在畢業的前夕讓你擔了，也謝謝你對我的鼓勵，You couldn't give up until the last day！！再來要感謝機械所徐文祥實驗室的學長們，讓我能順利完成實驗，也要謝謝交大奈中心的技術員，范秀蘭小姐和徐秀鑾小姐的代工幫忙，我才能順利畢業。

最後要謝謝實驗室的每一位，電鍍達人光哥、不再憂鬱的瑋哥、帶便當上學的川哥、BT 達人凱哥、最帥的達叔、製程達人子元、消失的胖子健章、褲底插針的 chando、十分有主見的思穎、Allen 的朋友昱文、還有剛升碩二的睿婉、濬誠、文駿、以及碩一的學弟們、最後當然是過很爽的助理小筑，謝謝你們囉，雖然我沒能為這個實驗室留下什麼，能留下的只有對各位的祝福，畢業的路看似漫長，但終點一直都在，NEVER GUVE UP！！

Contents

摘要 ..... **i**

Abstract ..... **ii**

Acknowledgments ..... **iii**

誌謝 ..... **iv**

Contents ..... **v**

Figure Captions ..... **vi**

Contents

Chapter 1 Introduction **1**

Chapter 2 Design and Analysis **4**

2.1 Design Concept of the Biomimetic Microphone 4

2.2 Finite Element Analysis 8

2.3 Fabrication Process of the Biomimetic Microphone 13

Chapter 3 Results and Discussions **15**

3.1 Result of the Optimum Design 15

3.2 Influence of the Serpentine Spring 16

3.3 Scanning Electro Microscope (SEM) Photographs 18

3.4 The Vibration Mode 19

Chapter 4 Summary and Future Work **21**

4.1 Summary 21

4.2 Future Work 21

References **22**

Figure Captions

Chapter 2

Fig. 2-1 A picture of the three leaves oxalis 4

Fig. 2-2 The design of the oxalis-like sensing diaphragm 5

Fig. 2-3 A schematic of the boundary condition with a pressure load applied at 0° in the ANSYS 7

Fig. 2-4 (a), (b) and (c) show the polar patterns of the net, ipsilateral, and contralateral displacement with Ono's design (blue line) and 4 leaves oxalis-like diaphragms (red line) 8

Fig. 2-5 The net displacement of the Ono's design with 3 inner and 3 outer beams The maximum displacement is about 0.737μm 10

Fig. 2-6 The net displacement of the Ono's design with 4 inner and 4 outer beams The maximum displacement is about 0.491μm. 11

Fig. 2-7 An optimum oxalis-like diaphragm with 6 inner and 6 outer supporting beams and each beam is 10μm wide and 65μm long. The thickness of sensing diaphragm is 5μm. 12

Fig. 2-8 Process flow of the biomimetic microphone 14

Chapter 3

Fig. 3-1 The analysis results of the proposed optimum oxalis-like biomimetic microphone 15

Fig. 3-2 The relation between the springs and beams 16

Fig. 3-3 Comparison the radius of the ring 17

Fig. 3-4 (a), (b), and (c) show the Scanning Electro Microscope (SEM) photographs 18
Fig. 3-5 (a), (b) and (c) show in-phase, y-axis and x-axis reversed-phase modes and their resonant frequencies 20

Chapter 1 Introduction

It had been a grand challenge to miniaturize a sound source localizing system due to minute interaural intensity and time differences occurring in its acoustic sensing components. Until 1992, the related acoustic sensing mechanism of small insect like parasitoid fly (Orima Ochracea) was fully investigated and realized that the interaction between ipsilateral and contralateral pressures can increase effective interaural distance via a mechanical intertympanal bridge structure that resulting in an expanded interaural time difference for locating the sound field [1,2]. In 2001, Yoo et al presented the first biomimetic microphone based on a hinge-supported diaphragm behaving like the intertympanal bridge for sound localization. They utilized DRIE (Deep Reactive Ion Etch) process to form a corrugated polysilicon diaphragm that attached with single crystal silicon proof masses and solid stiffeners on a SOI wafer for the fabrication of a directional microphone [3-5]. The developed technique can not only provide high design flexibility over conventional etch-stop approach but also simplify the fabrication of corrugate structure that designed for sensing diaphragm with better mechanical sensitivity. The microphone started realizing the possibility of directional hearing purpose for hearing aid application. Since then, a variety of biomimetic microphones with improved structural designs have been proposed and fabricated using silicon micromachining technology for better performance.

For example, Ono et al demonstrated a biomimetic microphone based on a center-supported gimbal circular diaphragm structure which provides a 360 degree of freedom for better directional identification with a spatial resolution as well as 15° [6-9]. Cui et al. implemented an integrated optical readout in the sensing membrane of the directional microphone. Via the diffraction-based optical interferometric detection, the device can avoid thermal noise problem imposed by capacitive sensing [10].

Meanwhile, for a hearing system, surrounding sound is first sensed and transformed into electrical signals via a microphone or microphone array. The electrical signals are then processed, amplified, and reformed by integrated signal processing chips. Finally, the reshaped electrical signals are transformed into an acoustic wave then transmitted into patient's eardrum via a microspeaker. Because the hearing aids must be portable and adaptive to satisfy the needs from a variety of patients, several characteristics including low powered, low noise, miniature, and programmable, must be included in the device design. In order to satisfy these requirements, the aforementioned micromachined biomimetic microphone for sound localization could play a key role in terms of low power, low noise, and small form factor criteria. As long as the origin of sound source can be located, the signal-to-noise ratio (SNR) of a certain acoustic sensor can be effectively enhanced by the noise source removal from the sensed signal since the other sound sources will be treated as background noise which can be

effectively eliminated via signal processing.

Nevertheless, the existing biomimetic microphones still exhibit several deficiencies, like the trade-off necessity of structural sensitivity and rigidity in Ono's design and process complexity increase for optical readout integration. Optimum design is still required for further applications. Therefore, in this paper, we will present a newly developed biomimetic microphone based on the combined structural of ormia ochracea and oxalis to further enhance the capability of sound source localization. Since the microphone can be fabricated using conventional surface micromaching process, low manufacturing and small form factor will make the device fascinating for hearing aid applications.

Chapter 2 Design and Analysis

2.1 Design Concept of the Biomimetic Microphone

The proposed microphone still follows the Ono's design with a gimbals-supported circular sensing diaphragm. The difference, however, is that a full circular diaphragm will be divided into several parts like oxalis leaves as shown in Fig. 1 which can increase the sensitivity in each sensing area due to the diaphragm disintegration. Meanwhile, for keeping the diaphragm vibrate in-phase and reversed-phase modes like the auditory organ of the parasitoid fly, the divided sensing diaphragms are connected to each other by serpentine springs. Fig. 2 depicts a whole structure of the microphone with a capacitive sensing design.

Fig. 2-1 A picture of the three leaves oxalis [11].

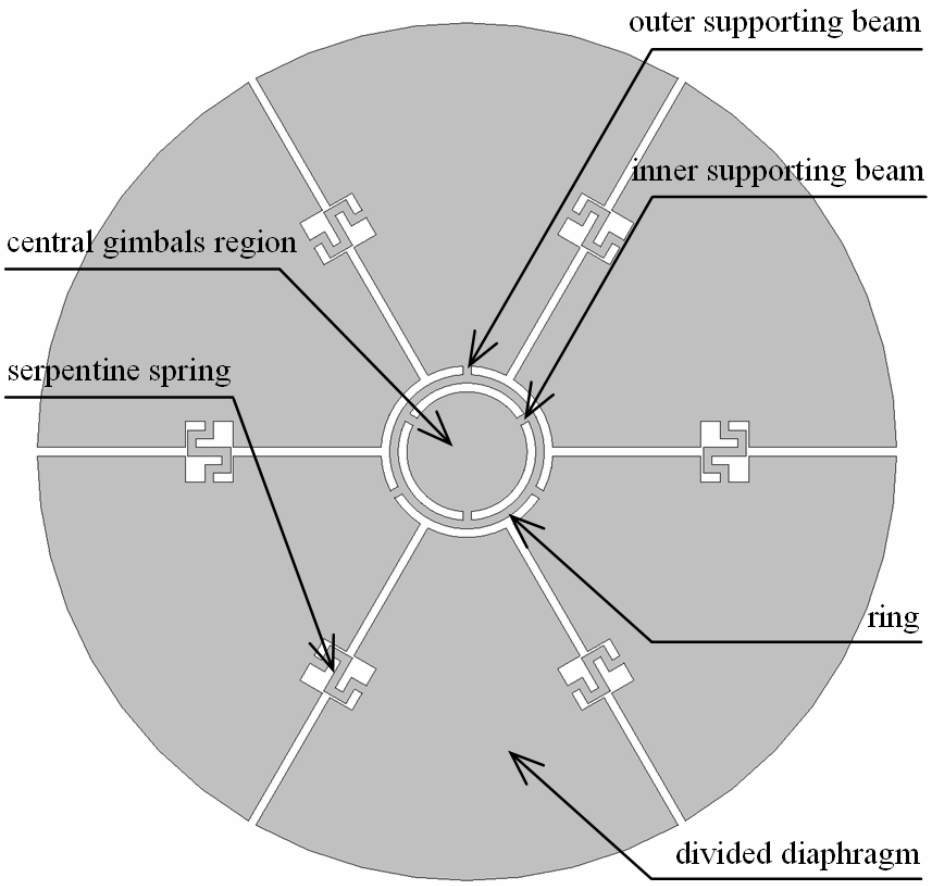

Fig. 2-2 The design of the oxalis-like sensing diaphragm

In the structure, sensitivity relies on the gimbals flexibility, the size of sensing leaf, and the spacing between the leaf and the number of the electrode underneath the sensing leaf. In order to improve the spatial resolution for sound localization, the simplest way is to increase the number of bottom electrodes which would result in the decrease of sensing area, i.e. the reduction of capacitance change (ΔC). In addition, since the circular diaphragm is an axial symmetry structure, simultaneously increasing the supporting beams is required at the central gimbals region for a symmetrical acoustic response at each sensing

leaf which would result in the decrease of sensitivity due to the increase of structural rigidity, i.e. the increase of effective spring constant of supporting beams. Thus, in this thesis, an optimum design of oxalis-like biomimetic microphone is analyzed and proposed in the following using ANSYS simulator [12]. In addition, because the sensitivity of a capacitive microphone is defined by mV/Pa which is contributed by the distance change between the sensing diaphragm and its bottom electrode that caused by applied sound pressure, we will use the maximum displacement of sensing diaphragm as an indicator for the microphone sensitive comparison in the following analysis.

As derived by beam theorem [13], the moments of inertia and the deflection of a cantilever beam while a force is applied on the edge of the beam can be calculated as the following equations

$$I = \frac{W_b t^3}{12} \quad \text{.....Eq.(1)}$$

$$d_B = \left(\frac{L_b{}^3}{3EI} \right) F \quad \text{.....Eq.(2)}$$

where E is the Young's Modulus, Lb is the length of the beam, Wb is the width of the beam, and t is the thickness. Combined with Eq.(1) and (2), we can get

$$F = k \times x_B = \left(\frac{EW_b t^3}{4L_b{}^3} \right) \times d \Rightarrow k = \frac{EW_b t^3}{4L_b{}^3} \quad \text{.....Eq.(3)}$$

From which, higher sensitivity could be realized with a larger deflection via

adjusting the length, width, and number of supporting beams to reduce the effective spring constant of the center-supported structure. For the structural sensitivity analysis, a 0.02Pa sound pressure load which is about 60dB SPL (Sound Pressure Level), the most comfortable sound volume for human beings, will be applied on the half of the sensing diaphragm at 0° as shown in Fig. 3 then the load will be rotated counter-clockwise for 360°.

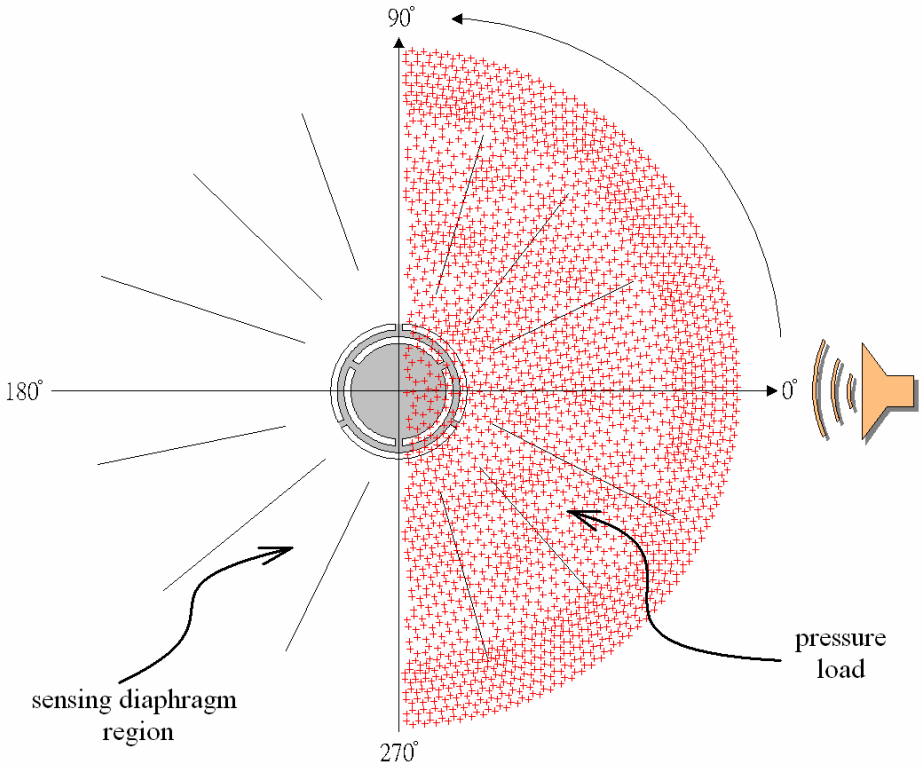

Fig. 2-3 A schematic of the boundary condition with a pressure load applied at 0° in the ANSYS.

2.2 Finite Element Analysis

Fig. 4 shows a normalized displacement comparison of sensing diaphragms between the Ono's design and the same design but with oxalis leaves in a polar pattern plot. The polar pattern plot is a logarithm of the normalized displacements which can also show the directivity of the microphone.

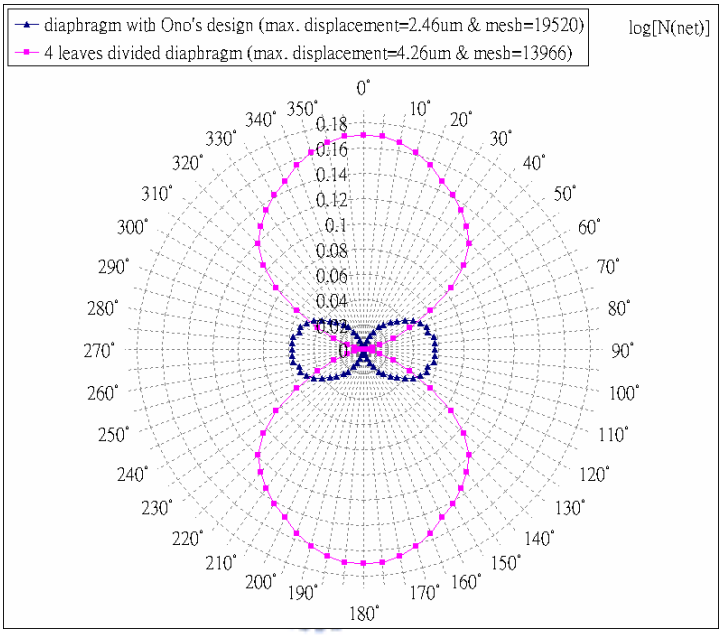

(a)

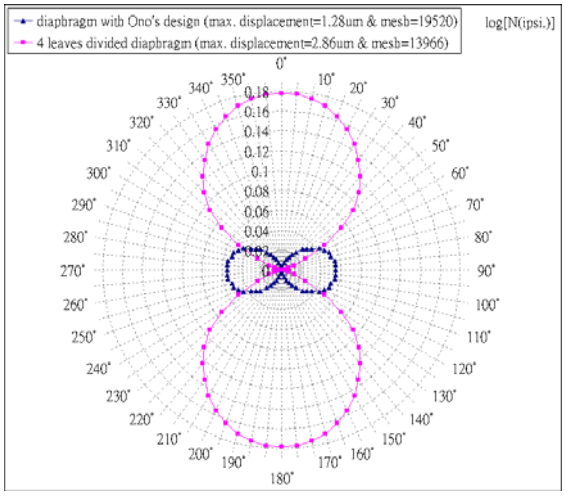

(b)

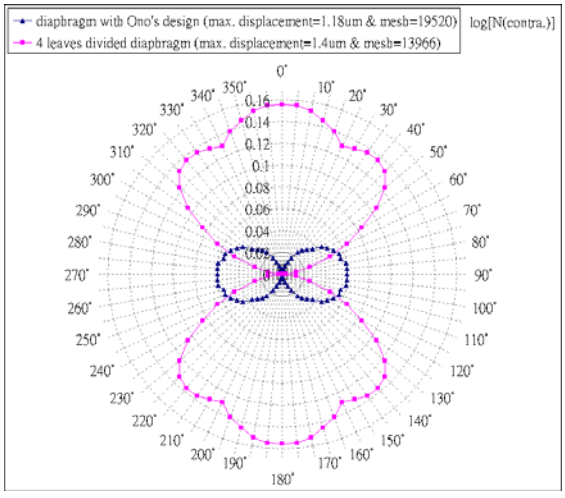

(c)

Fig. 2-4(a), (b) and (c) show the polar patterns of the net, ipsilateral, and contralateral displacement with Ono's design (blue line) and 4 leaves oxalis-like diaphragms (red line).

Fig. 4 depicts two kinds of sensed diaphragms which are based on the Ono's design and the oxalis-like design, respectively. Both central gimbals are designed with 2 inner and 2 outer pivots, 20μm wide, 65μm long, and 5μm thick supporting beams. The radius of diaphragms is 2500μm. The polar patterns shown in Fig. 4(a) indicate that the total displacement of the diaphragm with the oxalis-like design (red line) has 1.73 times larger than that of the diaphragm with the Ono's design (blue line) while a 0.02Pa pressure load is applied on the half of both diaphragms. Fig. 4(b) and (c) show the maximum displacements along ipsilateral and contralateral sides for each design, respectively. The maximum displacements of Ono's design are about 1.28μm in the ipsilateral side and 1.18μm in the contralateral side both occurring at 90° and 270°. The maximum displacements of oxalis design are about 2.86μm in the ipsilateral side and 1.4μm in the contralateral side both occurring at 0° and 180°. In the analysis, though the total amounts of mesh elements are not equal to each other due to the area difference between the Ono's and oxalis-like diaphragms, their mash sizes are controlled with the similar size. The disintegration designs indeed amplify the displacement of sensing diaphragm.

The two-fold symmetrical polar patterns shown in Fig. 4 also reveal an important message that the sensing response is directional dependent. An open area resulted by minute displacement is about 40°~50° wide. The opening will lessen the ability of microphone to sound localization in terms of limited spatial

resolution and it can be attributed to the non-axially symmetrical distribution of spring constant which can be resolved by increasing the number of the inner and outer beams. Figure 5 shows the polar pattern of the sensing diaphragm with the Ono's design under the same as the aforementioned loading condition. The opening angle can be effectively reduced from 40° to 20°. Meanwhile, it has been found that the opening angle can be reduced to 0° as shown in Fig. 6 once the number of total supporting beams has been increased to 8 or more that should be equally divided for the number of inner and outer supporting beam. Thus, the higher the number of supporting beam is, the smaller the opening angle will be, i.e. the better the spatial resolution will be.

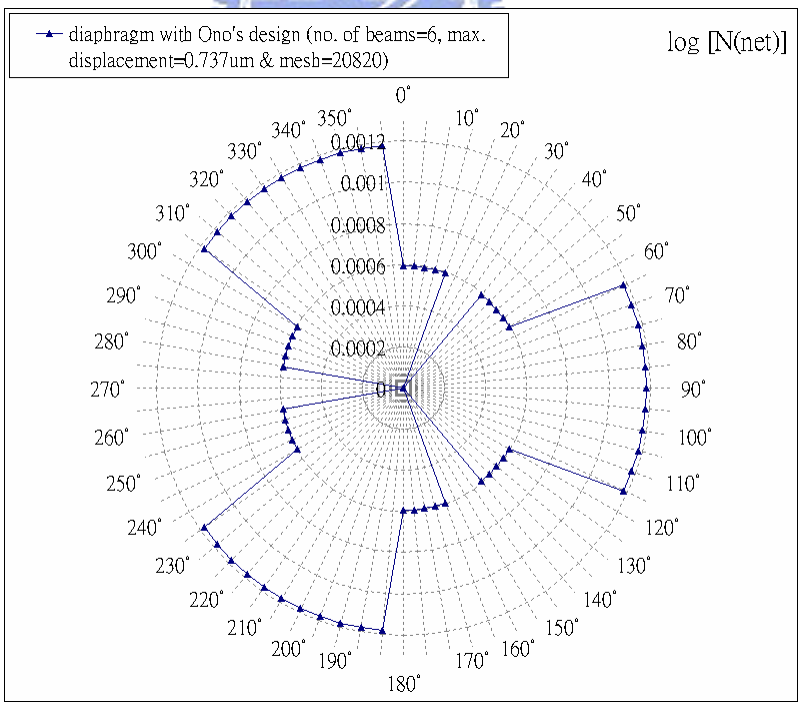

Fig. 2-5 The net displacement of the Ono's design with 3 inner and 3 outer beams The maximum displacement is about 0.737μm.

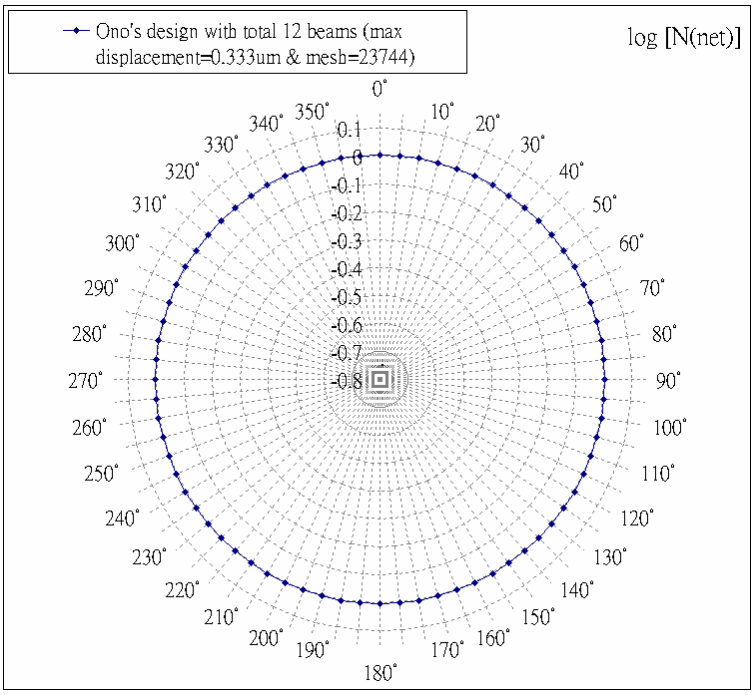

Fig. 2-6 The net displacement of the Ono's design with 4 inner and 4 outer beams The maximum displacement is about 0.491μm.

On the other hand, for the central supporting gimbals structure being loaded, the deformation will be concentrated at the regions of supporting ring and beams. When the number of inner and outer beams is increased for the reduction of opening angle, the effective spring constant would also be increased that will results in the reduction of the maximum displacement in the diaphragm structure. Thus, as shown in Fig. 5, the maximum displacement has been reduced from 2.46μm to 0.737μm although about 20° opening angle is reduced while the number of supporting beams increases from 4 to 6. Nevertheless, via an appropriate adjustment of the length, width, or thickness of the beam based on equation (3), the effective spring constant can still be kept at the same value even though the beam number is increased.

According to these analyses, a high performance biomimetic microphone should be designed with a center-supported circular microphone diaphragm being dissected into several parts like oxalis leaves, with a larger numbers of supporting beams with smaller width, thickness, or larger length, for maximizing its the sensitivity and spatial resolution. Fig. 7 shows an optimum oxalis-like biomimetic microphone which is designed with 6 leaves coupled with 6 serpentine springs, 6 bottom electrodes, and 12 supporting beams, which are 6 inner and 6 outer supporting beams, respectively. Each supporting beam is 10μm wide and 65μm long and each serpentine spring is 20μm wide and 300μm long in total. The thickness of sensing diaphragm is designed with 5μm.

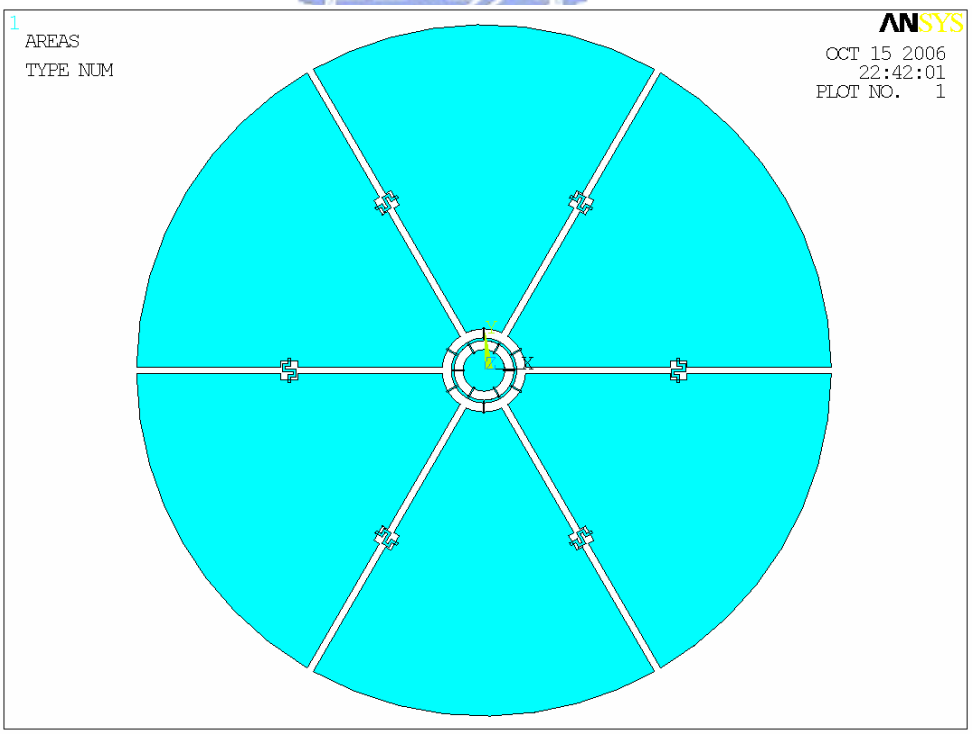

Fig. 2-7 An optimum oxalis-like diaphragm with 6 inner and 6 outer supporting beams and each beam is 10μm wide and 65μm long. The thickness of sensing diaphragm is 5μm.

2.3 Fabrication Process of the Biomimetic Microphone

The designed biomimetic microphone can be realized using a standard Multi-User MEMS Process (MUMP) with three poly-silicon layers and two sacrificial layers. Fig. 8 shows process flow for the microphone fabrication.

Step1: After standard RCA clean, a 4" silicon wafer is deposited with 0.6μm thermal wet oxidation at 1050°C and 0.6μm LPCVD low stress Si3N4 at 850°C for electrical isolation.

Step2: A 0.5μm LPCVD N-type doped poly-Si is deposited at 585°C and patterned as the bottom sensing electrode (Fig. 8a).

Step3: A 2μm thick HDPCVD SiO2 is deposited at 300°C and patterned as the first sacrificial layer (Fig. 8b).

Step4: In order to realize the center supporting structure, the second layer of heavily doped poly-Si is deposited and etched (Fig. 8c).

Step5: The second sacrificial layer of 0.75μm thick HDPCVD SiO2 is deposited and etched (Fig. 8d).

Step6: Finally, the 1.5μm heavily doped poly-Si diaphragm is deposited by LPCVD and etched (Fig. 8e).

Step7: The last step is release the diaphragm by B.O.E. wet etching (Fig. 8f).

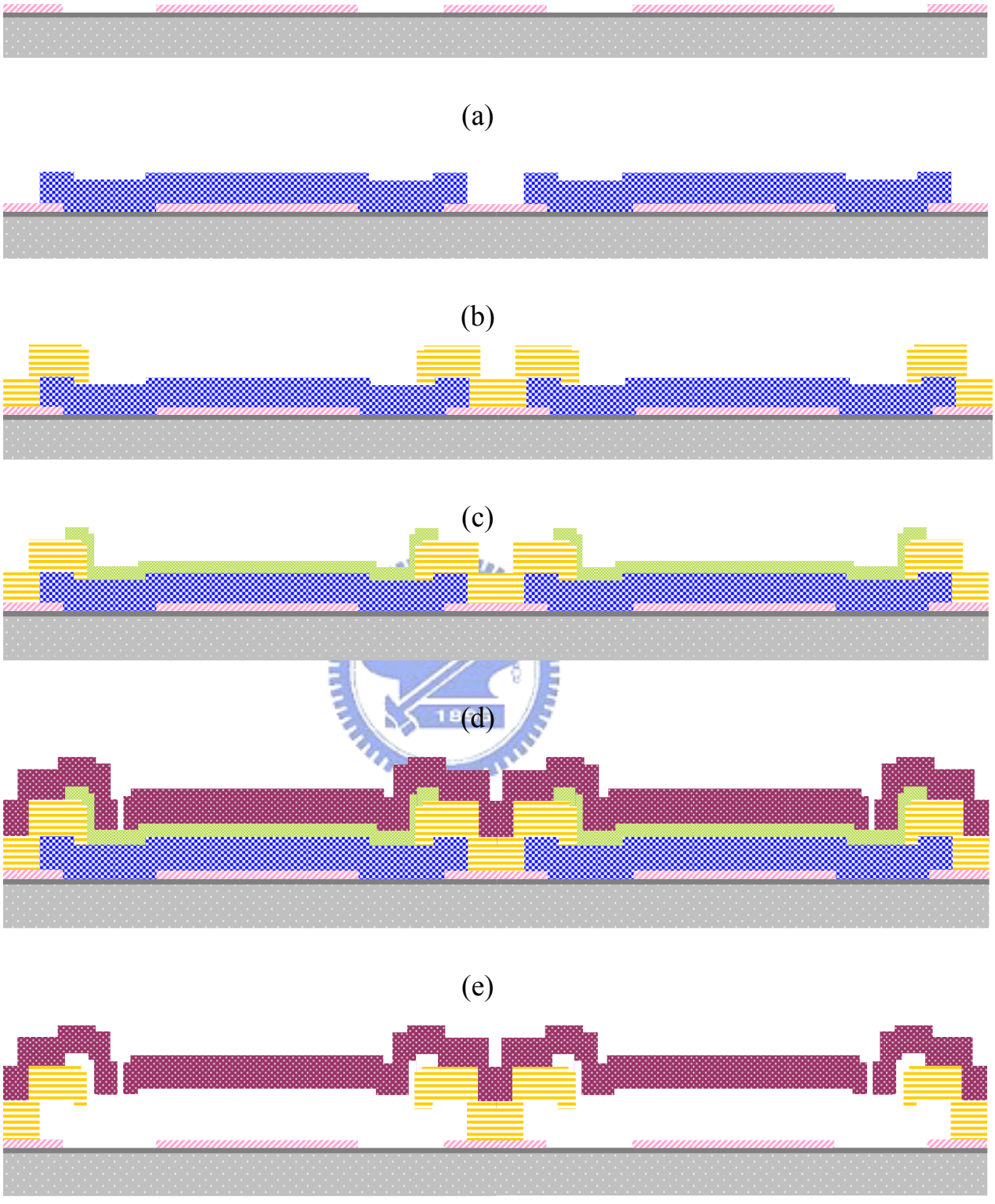

Fig. 2-8 Process flow of the biomimetic microphone

Chapter 3 Results and Discussions

3.1 Result of the Optimum Design

Fig. 9 shows the analysis results of the proposed optimum oxalis-like biomimetic microphone. The maximum net displacement is about 1.267μm and the opening angle is only 10°. In the design, the higher the number of sensing leaf is, the better the spatial resolution will be. Nevertheless, instead of 8 or more sensing leaves, the number of 6 is determined by the minimum sensing capacitance which depends on the sensing circuit limitation. Since the minimum detected capacitance change is proportional to the overlapped area between the top sensing diaphragm and the bottom electrode, the area cannot be infinitesimal due to the limitation of S/N ratio (Signal-to-Noise ratio) of sensing circuit. The leaf number is restricted. shown in the Fig. 9 and Fig. 10.

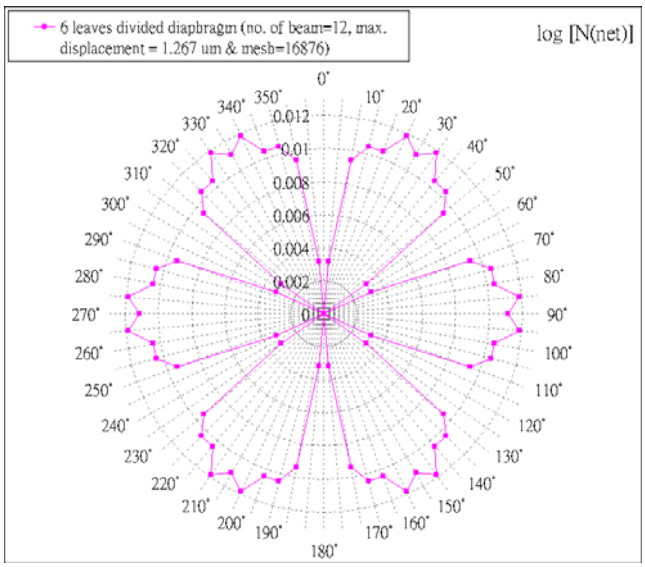

Fig. 3-1 The analysis results of the proposed optimum oxalis-like biomimetic microphone

3.2 Influence of the Serpentine Spring

In addition, for a six-leaves diaphragm design, the number of total supporting beams can be 6 or more. However, in order to ensure a symmetrical acoustic response, each sensing leaf is designed to connect a supporting beam, i.e. outer supporting beam. Therefore, a total 12 supporting beams are designed. However, in comparison with the aforementioned Ono's design with more than 8 supporting, the oxalis-like diaphragm design still exhibit a 10° opening even though the diaphragm has better displacement performance. Since the opening could be related to the disintegration design, the coupling springs can be modified from a serpentine shape into a simple beam design but with the same width and thickness. Fig. 10 shows that about 2° open angle reduction can be realized. Because the diaphragm becomes more rigid due to stronger coupling, the net displacement has been reduced from 1.267μm to 1.245μm which is 3.7 times larger than that with Ono's design (0.333μm).

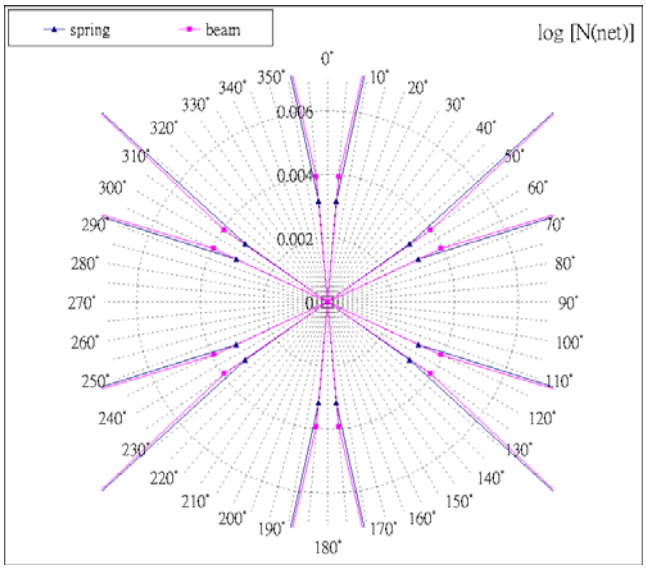

Fig. 3-2 The relation between the springs and beams

Moreover, in the Fig. 9, each polar pattern is not smooth enough that will make some errors for sensing circuit caused by the same sound pressure with different response. We need to improve the oxalis-like biomimetic diaphragm. Therefore, we adjust the position of the ring with different radius and the ring is designed with 20μm wide. If we move the ring outward, i.e. the length of the inner beam (100μm) is longer than outer beam (30μm), the polar pattern becomes smoother (red line). Oppositely, if we move the ring inward with 30μm long inner beam and 100μm long outer beam, the polar pattern is rough (blue line). The result is shown in Fig. 11. Meanwhile, the net displacement is reduced when moving the ring outward. According to the beam theorem and stress concentration, the loaded leaf applies a force on the shorter beam, i.e. the effect spring constant is larger than longer one, and the displacement will be reduced. However, the net displacement is still larger than Ono's design.

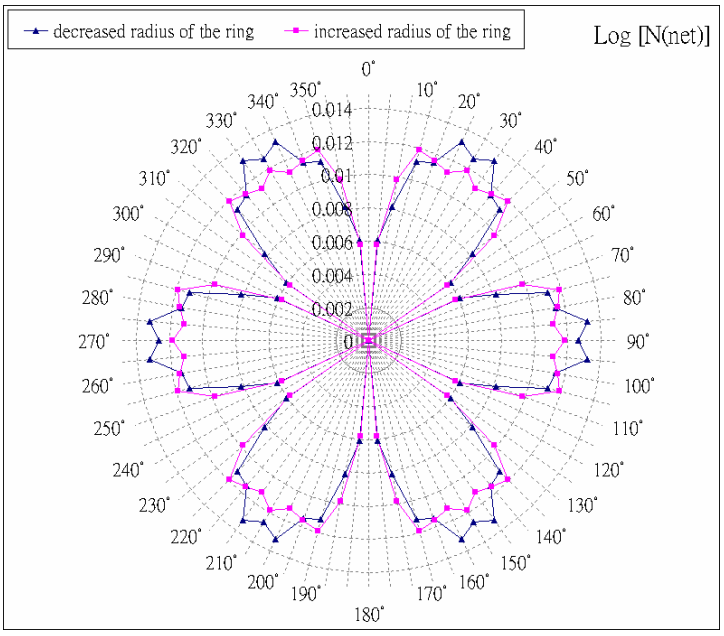

Fig. 3-3 Comparison the radius of the ring

3.3 Scanning Electro Microscope (SEM) Photographs

Fig. 12(a), (b), and (c) depict the Scanning Electro Microscope (SEM) photographs of the oxalis-like sensed diaphragm, and the enlarged view of the serpentine spring and the central gimbals region, respectively. In order to release more easily, we arrange the layout of etching holes which the diameter is 10μm and the distance between each hole is 40μm on each leaf. The performance and reliability of the oxalis-like sensing diaphragm will be affected due to the limitation of the instrument, such as the over etching by RIE and the surface roughness by LPCVD.

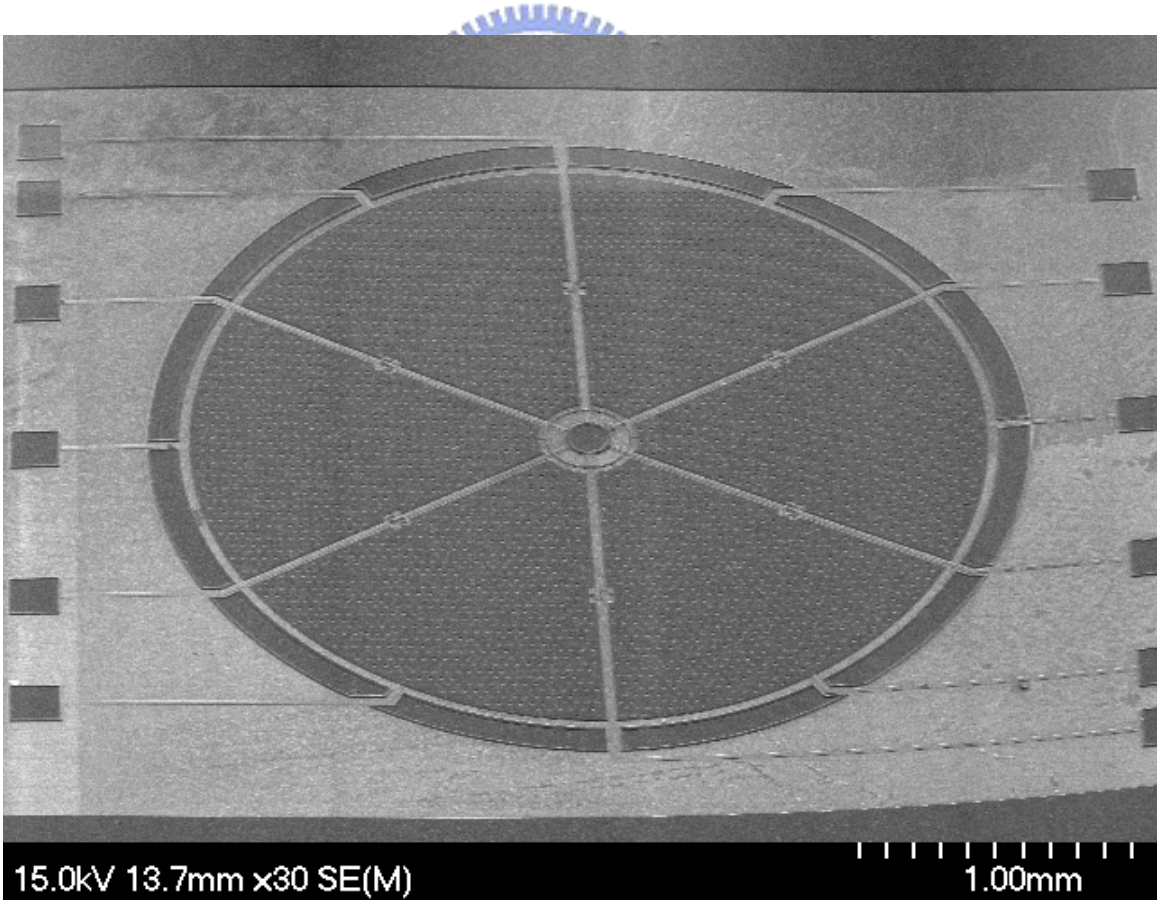

(a)

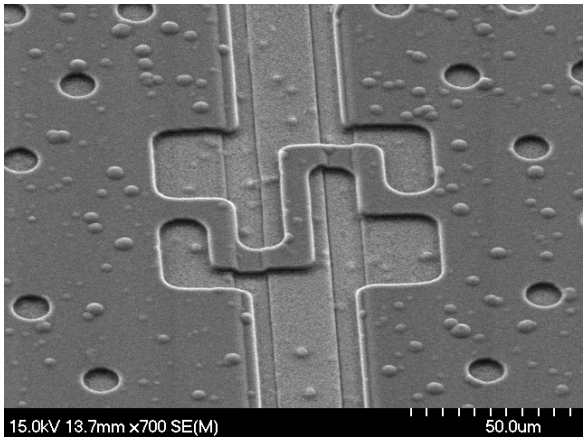

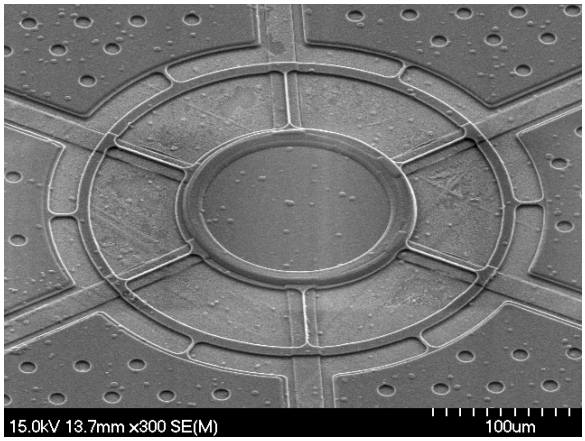

(b) (c)

Fig. 3-4 (a), (b), and (c) show the Scanning Electro Microscope (SEM) photographs of the oxalis-like sensed diaphragms, ant the enlarged view of the serpentine spring and the central gimbals region, respectively.

3.4 The Vibration Mode

In Fig. 4(b) and (c), we find the ipsilateral and contralateral sides vibrate the opposite direction (reversed-phase vibration mode) when a pressure difference between the two sides of the divided diaphragm. Nevertheless, the ratio between the ipsilateral and contralateral displacements is not approach to unity. This problem can be solved by designing the size of the MOS-FET in the differential amplifier circuit. Furthermore, because of the serpentine springs, the oxalis-like diaphragm can vibrate in-phase and reversed-phase modes like the auditory organ of the parasitoid fly. Thus, we use the ANSYS to simulate the modal analysis to obtain the resonant frequencies, and show the in-phase, y-axis and x-axis reversed-phase vibration modes which their resonant frequencies are

256.998 Hz, 261.751 Hz and 261.945 Hz respectively. The displacement of the diaphragm along z-axis is represented by different color in Fig. 13.

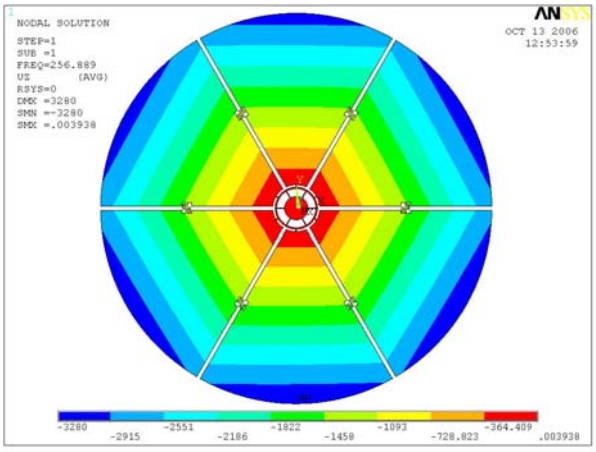

(a)

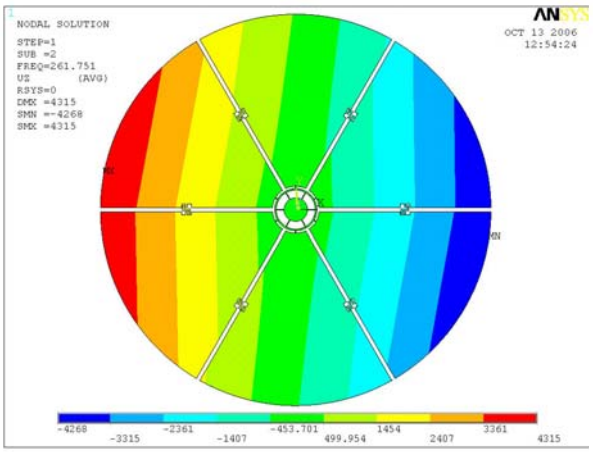

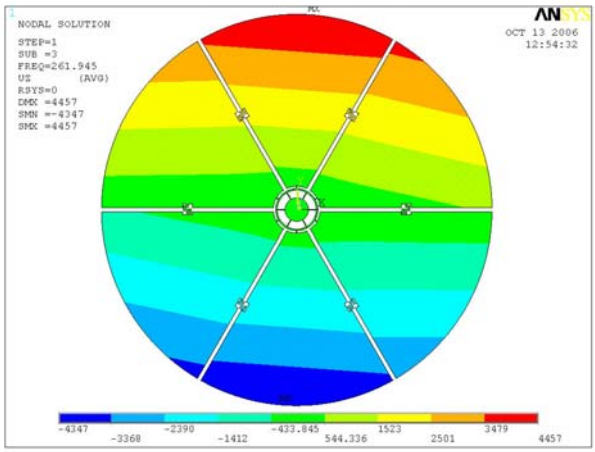

(b) (c)

Fig. 3-5(a), (b) and (c) show in-phase, y-axis and x-axis reversed-phase modes and their resonant frequencies are 256.998 Hz, 261.751 Hz and 261.945 Hz respectively.

Chapter 4 Summary and Future Work

4.1 Summary

A newly developed micromachined biomimetic microphone by utilizing the central gimbals-support circular structure [5-8], and mimicking the structure of the oxalis is proposed. The net displacement of the diaphragm with the oxalis-like design is 3.7 times larger than that of the diaphragm with the central gimbals-support circular diaphragm design, and the oxalis-like diaphragm performs the spatial resolution with opening angle smaller than 10 degrees. Therefore, the oxalis-like diaphragm can not only improve the displacement by decoupling the sensing diaphragm but also enhance the capability of sound source localization with the optimum design of the central gimbals structure. The design and FEM simulation are analyzed by ANSYS simulator. The process of the single-wafer biomimetic microphone is fabricated by the standard Multi-User MEMS Processes (MUMPs) with three poly-silicon layers and two sacrificial layers.

4.2 Future Work

We need to verify the FEM analysis and the experimental result via the acoustic measurement system and realize the integration of the biomimetic microphone and CMOS circuit for low power hearing aid application.

References

[1] D. Robert, J. Armoroso, and R. R. Hoy, “The Evolutionary Convergence of Hearing in a Parasitoid Fly and Its Cricket Host,” Science, Vol. 258, pp. 1135-1137, Nov. 1992.

[2] R. N. Miles, D. Robert, and R. R. Hoy, “Mechanically coupled ears for directional hearing in the parasitoid fly Ormia ochracea,” J. Acoust. Soc. Am, Vol. 98, No. 6, pp. 3059-3070, Dec. 1995.

[3] Kyutae Yoo, J.-L. A. Yeh, N. C. Tien, C. Gibbons, Q. Su, W. Cui, and R. N. Miles, “Fabrication of a Biomimetic Corrugated Polysilicon Diaphragm with Attached Single Crystal Silicon Proof Masses,” Solid-State Sensors and Actuators, Transducers’01, pp. 130-133, Jun. 2001.

[4] K. Yoo, C. Gibbons, Q.T. Su, R.N. Miles, and N.C. Tien, “Fabrication of Biomimetic 3-D structured Diaphragms,” Sensors and Actuators A, Vol. 97-98, pp. 448-456, Apr. 2002.

[5] Kyutae Yoo, Quang Su, Ronald N. Miles, and Norman C. Tien “Biomimetic Direction-Sensitive MicroMachined Diaphragm for Ultrasonic Transducers,” IEEE Ultrasonics Symposium, Vol. 2, pp. 887-890, Oct. 2001.

[6] Akihito Saito, Nobutaka Ono, and Shigeru Ando, “Micro Gimbal Diaphragm for Sound Source Localization with Mimicking Ormia Ochracea,” SICE, Vol. 4, pp. 2159-2162, Aug. 2002.

[7] Nobutaka Ono, Akihito Saito, and Shigeru Ando, “Design and Experiments of Bio-mimicry Sound Source Localization Sensor with Gimbal-Supported Circular Diaphragm,” Solid-State Sensors and Actuators, Transducers’03, pp. 939-942, Jun. 2003.

[8] Nobutaka Ono, Akihito Saito, and Shigeru Ando, “Bio-mimicry Sound Source Localization with Gimbal Diaphragm,” T.IEE Japan, Vol. 123-E, No. 3, pp. 90-97, Mar. 2003.

[9] N. Ono, T. Arita, Y. Senjo, and S. Ando, “Directivity Steering Principle for Biomimicry Silicon Microphone,” Solid-State Sensors and Actuators, Transducers’05, pp. 792-795, Jun. 2005.

[10] Weili Cui, Baris Bicen, and Neal Hall, “Optical Sensing in a Directional MEMS Microphone Inspired by the Ears of the Parasitoid Fly, Ormia Ochracea,” IEEE international Conference on MEMS, pp. 614-617, Jan. 2006.

[11] http://aiforum.cse.ttu.edu.tw/plant/guide.htm

[12] ANSYS, http://www.ansys.com/ 9.0 version

[13] Roy R. Craig, Jr. Mechanics of Materials, 2nd New York: Wiley, 1999

Vita

姓　　名：景文澔 (Wen-Hao Ching)

出生日期：中華民國七十一年四月十九日

出 生 地：台北市

E - mail：howardching.ee93g@nctu.edu.tw

學　　歷：

台北市立復興高級中學　(1998.9～2000.6)
(Taipei Municipal Fu-Hsing Senior High School)

國立中央大學電機工程學系　(2000.9～2004.6)
(Department of electrical Engineering, Nation Central University)

國立交通大學電子工程所碩士班　(2004.9～2006.10)
(Department of electronics Engineering & Institute of Electronics, Nation Chiao-Tung University)